Low-Boom Design of a T-tail Supersonic Transport Configuration

Qing Chen[1,2], Zhonghua Han[1,2,*], Yulin Ding[1,2], Jianling Qiao[1,2], Ke Song[1,2], Wenping Song [1,2]

[1]Institute of Aerodynamic and Multidisciplinary Design Optimization, School of Aeronautics, Northwestern Polytechnical University, Xi'an, Shanxi 710072, People's Republic of China
[2]National Key Laboratory of Science and Technology on Aerodynamic Design and Research, Xi'an, Shanxi 710072, People's Republic of China
Hanzh@nwpu.edu.cn

Abstract. Sonic boom remains the primary bottleneck restraining commercial supersonic overland flight. However, designing a low-boom supersonic transport configuration with high aerodynamic efficiency is still a significant challenge. To address this problem, a baseline configuration with both low-boom and low-drag features is initially designed. Subsequently, low-boom inverse design and manual design are carried out successively. Regarding the inverse design, JSGD (Jones-Seebass-George-Darden) method is used to decrease the overpressure amplitude rapidly, while mixed-fidelity method is adopted to reduce the loudness to a lower level, where the target with volume and lift constraints is generated by PNFO (parameteric near-field pressure) method. For manual design, the flow field of aft-body region is analysed for the design of aft-body components. By adjusting the shape and position of T-tail, the shocks interfere with expansion waves beneficially, which smooths the pressure recovery of ground signature. Compared to baseline configuration, under the premise of maintaining cabin volume and cruise lift, design configuration exhibits more moderate near-field and far-field signatures. The undertrack ground loudness is reduced from 91.43 PLdB to 79.88 PLdB. Besides, full-carpet sonic boom intensity is significantly mitigated, with the lowest ground loudness of 77.88 PLdB recorded at the lateral cutoff angle. Additionally, the cruise lift-to-drag ratio is increased from 8.44 to 8.61. The configuration proposed in this paper can serve as a platform for researches of other supersonic transport technologies in the future.

Keywords: Supersonic Transport, Sonic Boom Prediction, Low-boom Design, Inverse Design Method, Tail-shock Reduction.

1 Introduction

Supersonic transport (SST) is one of the main focuses for the development of next-generation civil aircraft since it can significantly improve travel efficiency [1]. Concorde and Tupolev Tu-144 were once capable of commercial supersonic operations, but eventually retired due to serious environmental compatibility issues [2]. In recent years,

the call for the reintroduction of SST has been increasing. For example, NASA divides the development of SST into three stages: "N+1", "N+2" and "N+3", and the corresponding models are scheduled to enter service before 2035 [3]. Several institutions around the world have carried out researches on it and many configurations have been promoted [4]. However, sonic boom is still the core problem prohibiting the commercial supersonic overland flight. Hence, reducing sonic boom to a community-acceptable level is the critical technology for the design of SST.

To address this problem, The research of sonic boom has been going on internationally for seven decades and has led to the development of a series of sonic boom prediction and low-boom design methods [5]. Especially, the design of low-boom configuration has made significant progress in the past decade. For example, a low-boom S4 airliner with aerodynamic engine-airframe integration were designed by JAXA and its operational and economic assessments have been done by DLR [6]. Li and Geiselhart [7]developed a block coordinate optimization method for multidisciplinary design optimization and designed a configuration with various mission constraints. Ding [8]proposed an inverse design method with volume and lift constraints, and applied it to the design of a large SST named NPU-T7106. NASA's X-59 low-boom demonstrator has been underwent extensive researches and will be flown over communities to collect data from residents responding to the shaped sonic boom [9]. However, the ground loudness of the first three configurations is higher than 85 PLdB, the boom of X-59 is weak (about 75 PLdB) but the aerodynamic efficiency is relatively low. This means designing a low-boom configuration with excellent aerodynamic performance remains a significant challenge. Therefore, a low-boom SST configuration with high aerodynamic efficiency is designed in this paper, which can serve as a platform for subsequent researches of other SST technologies.

2 Methodology

2.1 Sonic Boom Prediction Method

Sonic boom prediction is the cornerstone of low-boom design. The prediction method used in this paper is shown in Fig. 1. During the JSGD design phase, FA-Boom [10], a program based on modified linear theory [11][12], is used for near-field sonic boom rapid prediction. Considering the limitations of the modified linear theory, CFD simulation is used for the undertrack pressure analysis in mixed-fidelity design. In order to capture shocks and expansion waves accurately, a hybrid grid is used, comprising a cylinder block and a cone block. The governing flow equations solved are RANS (Reynolds-Averaged Navier-Stokes) equations with the SA turbulence model. The temporal discretization uses the LU-SGS implicit scheme, and the spatial discretization adopts the Roe upwind scheme with a minmod limiter. The prediction of far-field sonic boom utilizes an in-house code named bBoom [13][14], which simulates the propagation of sonic boom in the atmosphere by solving the augmented Burgers' equation. After the propagation of near-field signatures to the ground, Mark VII method developed by Stevens [15]is used to be the primary acoustic metric.

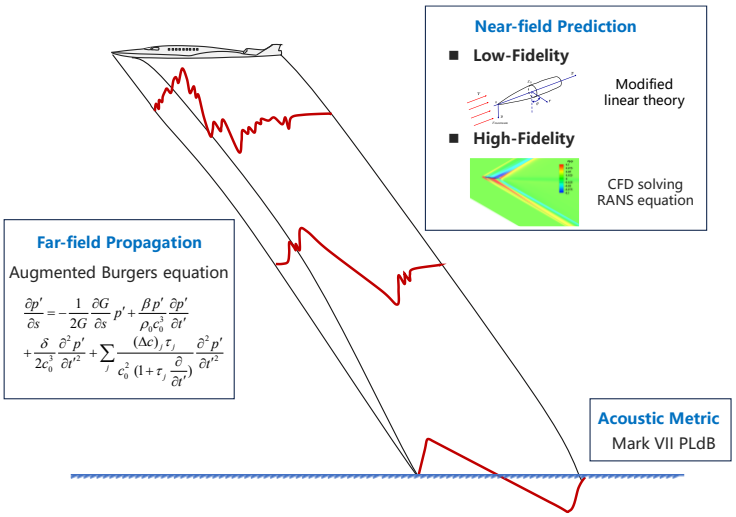

Fig. 1. Sonic boom prediction method used in this paper

2.2 Low-boom Design Method

The low-boom design method adopted in this paper involves two steps: inverse design of fuselage and manual design of aft-body component. The low-boom design flowchart is illustrated in Fig. 2.

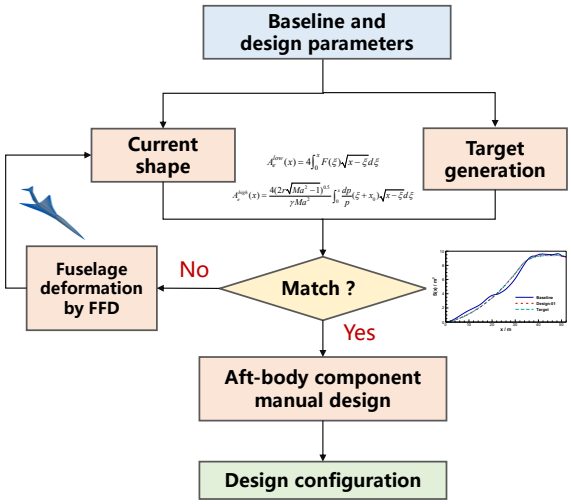

Fig. 2. Low-boom design process

Regarding the first step, JSGD inverse design [16]-[19] and mixed-fidelity inverse design (using an improved method considering volume and lift constraints [8]) are carried out respectively. During this stage, the target F function or target sonic boom signature

is converted into the area distribution, which is used to adjust the current shape until the design result matches target. At the second step, the shape and position of T-tail is designed manually to mitigate the intensity of sonic boom generated by aft-body [4].

3 Low-boom Design of T-tail SST Configuration

3.1 Design of Baseline Configuration

The baseline configuration with both low-boom and low-drag characteristics is designed at first. As shown in Fig. 3, the baseline features a slender fuselage, highly swept-back dihedral arrow wing, blunt leading-edge airfoil, and T-tail.

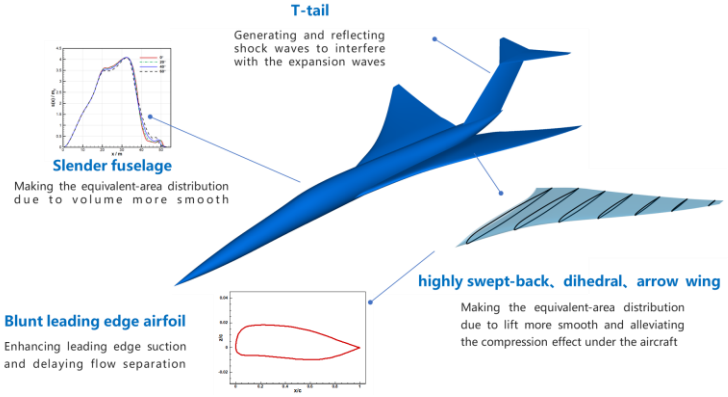

Fig. 3. Features of baseline configuration

Specifically, the slender fuselage allows for a smoother longitudinal volume distribution of the aircraft, which reduces the monopole effect of sonic boom and decreases the wave drag due to volume. The highly swept-back and dihedral arrow wing smooths the longitudinal lift distribution, mitigating compressibility effects. Hence, the dipole effect of sonic boom and wave drag due to lift can be reduced. The blunt leading-edge airfoil generates a strong leading-edge suction, which can reduce the pressure drag by delaying the flow separation. Besides, the leading edge of T-tail can generate shocks and the lower surface can reflect shocks. These shocks will have beneficial interference with the expansion waves, weakening the intensity of sonic boom generated by aft-body. The main design parameters of the baseline configuration are listed in Table 1.

Table 1. Parameters of the baseline configuration

Parameter	Value	Parameter	Value
Fuselage length	45 m	Cruise Mach number	1.6
Wing area	130 m^2	Cruise C_L	0.112
Take-off weight	300,000 N	Cruise altitude	16,000 m

3.2 Low-Boom Design

Fig. 4(a) illustrates the matching between the designed equivalent area distribution and target generated by JSGD theory. Fig. 4 (b) displays the comparison between the designed far-field signature and target generated by PNFO method. It can be observed that the designed results and targets coincide well, demonstrating the successful implementation of inverse design process.

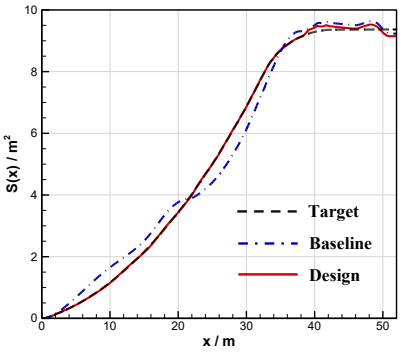

(a) Equivalent area distributions of target and design (JSGD inverse design)

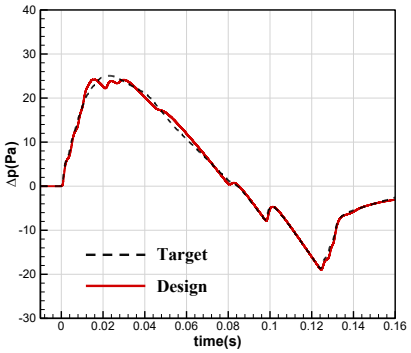

(b) Far-field signatures of target and design (mixed-fidelity inverse design)

Fig. 4. Comparison of target and design for inverse design

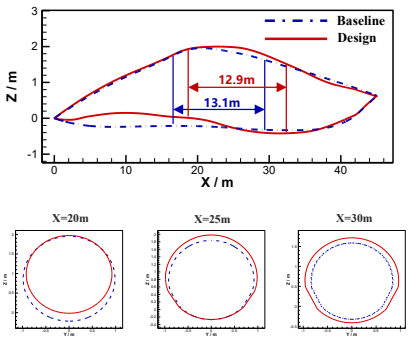

(a) Comparison of cabins between baseline and design configuration

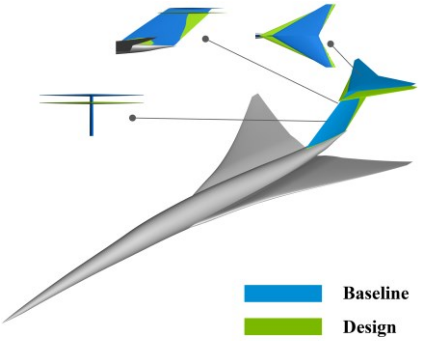

(a) Comparison of T-tails between baseline and design configuration

Fig. 5. Comparation of shapes between baseline and design configuration

Fig. 5 depicts the comparation of shapes between baseline and design configuration. Fig. 5(a) evidently presents that front and rear fuselage shrink while the middle fuselage expands, and the fuselage cabin section is basically maintained owing to the volume constraint imposed on the target generated by PNFO method. It is shown in Fig. 5 (b) that the leading edge of designed T-tail is moved forward and the trailing edge is moved backward, meanwhile the height is 0.43 m lower than baseline.

3.3 Analysis of Design Configuration

Near-field Sonic Boom Analysis

Near-field sonic boom can be obtained by solving RANS equations with 33.5 million cells. It can be observed from Fig. 6(a) that the contour of the design configuration is smoother and more dispersed, which means sonic boom intensity has been mitigated.

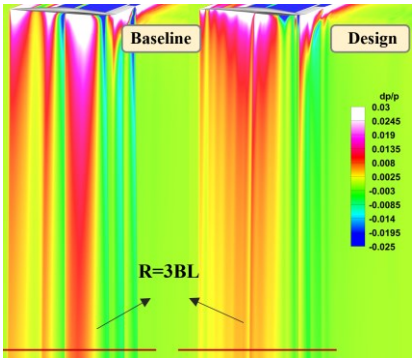

(a) Comparison of dp/p contours on the symmetric panel

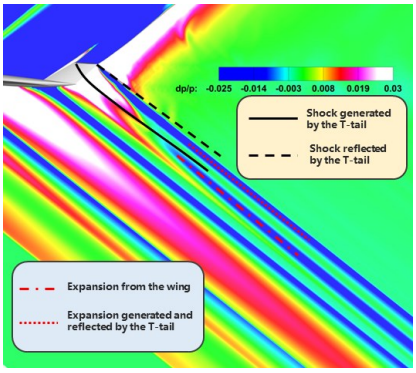

(b) Flow field of the aft-body region (baseline)

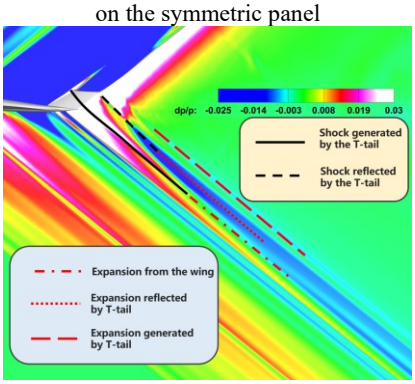

(c) Flow field of the aft-body region (design)

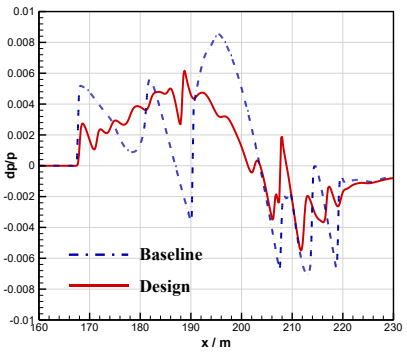

(d) Comparison of near-field signatures at 3 body lengths

Fig. 6. Comparison of near-field sonic boom characteristics

Fig. 6 (b) and (c) illustrate the comparison between the flow fields before and after the design. The shock waves generated by the baseline T-tail does not interfere beneficially with the expansion waves generated by the aft-body. However, in the flow field of design configuration, the designed T-tail generates and reflects shocks wakening the expansion waves from the wing.

Fig. 6 (d) presents a comparison of near-field sonic boom signatures at 3 body lengths. The low-boom design results in a significant decrease in the overpressure amplitude and more moderate change of pressure. Therefore, the near-field signature of design configuration consists of a series of weaker shock waves.

Far-field Sonic Boom Analysis

Based on the augmented Burgers equation, undertrack near-field signatures shown in Fig. 6 are propagated to the ground at an altitude of 16 km. Atmosphere conditions for sonic-boom propagation are standard atmosphere and relative humidity profile. Sampling frequency is 800 KHz and ground reflection factor is 1.9. Fig. 7 illustrates the evolution of sonic boom signatures in the atmosphere for baseline and design configurations. It is shown that the waves of the baseline configuration have already merged sufficiently when it propagates to 3 body lengths. As a result, the signature maintains strong shocks when it reaches ground. However, waves generated by the design configuration merge slowly in the atmosphere, eventually forming a smoother waveform on the ground.

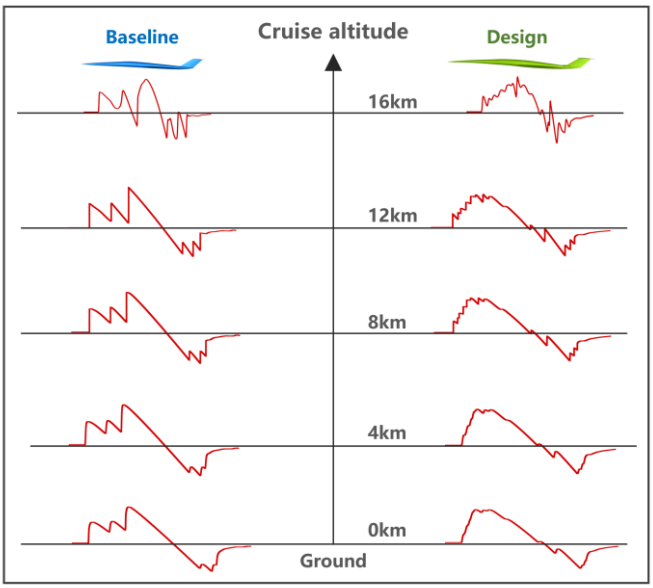

Fig. 7. Evolution of sonic boom signatures in the atmosphere

The ground loudness of baseline and design configurations evaluated by different metrics are listed in Table 2, and results show that undertrack loudness is reduced at all metrics. Consistent with international mainstream researches, PLdB is used as the primary metric hereinafter.

Table 2. Comparison of ground loudness using different acoustic metrics

Config.	PLdB	ASEL dB	CSEL dB
Baseline	91.43	77.69	95.92
Design	79.88	65.74	92.72

As shown in Fig. 8(a), for ground signature of the design configuration, the maximum overpressure is reduced and shock waves rise more gradually, resulting in a waveform closer to a sine wave. Fig. 8(b) presents a comparison of frequency spectrums. The design configuration has a significant decrease in medium and high frequency component components, fetching a ground loudness reduction of 11.55 PLdB.

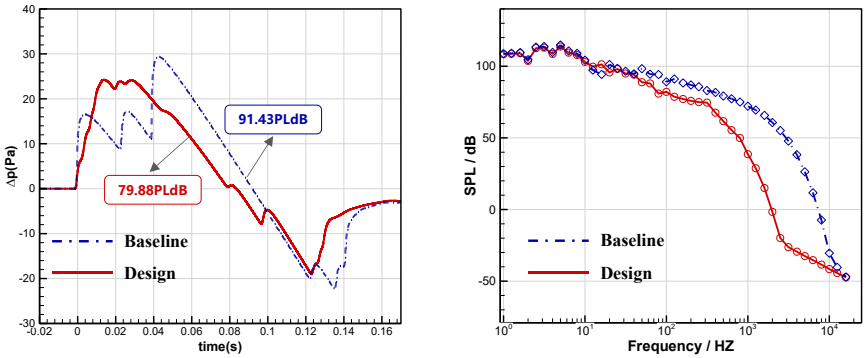

(a) Comparison of ground signatures (b) comparison of frequency spectrums

Fig. 8. Comparison of far-field sonic boom characteristics

Full-carpet Sonic Boom Characteristics

The sonic boom intensity distribution on the carpet is obtained by calculating the perceived sound pressure level of ground signatures at different azimuth angles.

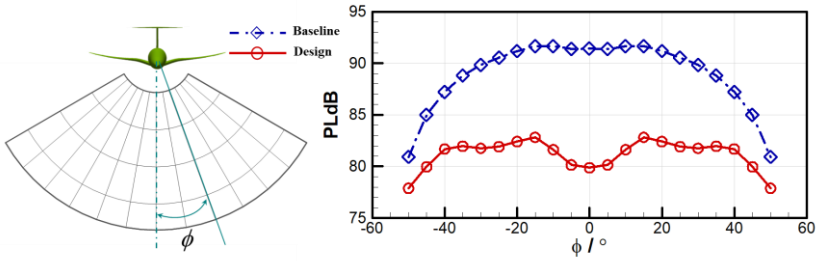

Fig. 9. Comparison of PLdB at different azimuth angle on the boom carpet

It can be observed from Fig. 9 that ground loudness is significantly reduced throughout the whole boom carpet. Specifically, the lowest sonic boom intensity is found near the lateral cutoff angle, measuring a loudness of 77.88 PLdB. When the azimuth angle is 15°, the highest loudness of ground sonic boom is recorded, reaching 82.82 PLdB.

Aerodynamic Performance

Lift and drag coefficients of the baseline and design configuration at cruise are listed in Table 3. It can be seen that both pressure drag and friction drag is reduced, as the wetted area of the fuselage is decreased and the shock wave is weakened during the low-boom

design process. Such drag reduction results in lift-to-drag ratio increasing from 8.44 to 8.61.

Table 3. Comparison of lift and drag coefficients at cruise

Config.	C_L	C_{Dp} (counts)	C_{Df} (counts)	C_D (counts)	L/D
Baseline	0.112	69.6	63.1	132.7	8.44
Design	0.112	68.7	61.4	130.1	8.61

The lift-to-drag characteristics of baseline and design configuration are compared in Fig. 10. Apart from the cruise C_L, the lift-to-drag ratio has also been improved in the vicinity of the design point. Besides, considering the cruise Mach number is 1.6, the cruise efficiency factor of the design configuration is 13.78.

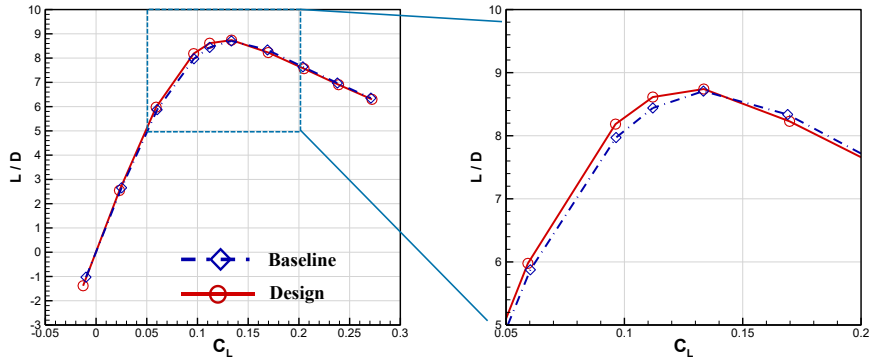

Fig. 10. Comparison of lift-to-drag ratio curves

4 Conclusion

This paper conducted a low-boom design research and a low-boom supersonic transport configuration with high aerodynamic efficiency is proposed, whose undertrack ground loudness is 79.88 PLdB and lift-to-drag ratio at cruise reaches 8.61. The inverse design method can effectively mitigate the overall intensity of the sonic boom. However, for aft-bodies with complex flow fields, it is necessary to carry out special designs focusing on the aft-body components. This can be achieved through manual design based on flow field characteristics or utilizing design optimization based on CFD. Owing to the aerodynamic design of baseline and the drag reduction during the low-boom design process, the proposed configuration exhibits good aerodynamic performance. Furthermore, future research will be conducted on full-carpet low-boom design, and provides a more comprehensive investigation on this design configuration, such as effects of propulsion systems on sonic boom and aerodynamic characteristics at low-speed.

References

1. Han, Z.-H., Qian, Z.-S., Qiao, J.-L.: Sheng bao yu ce yu di sheng bao she ji Fang Fa. 1st edn. Science Press, Beijing (2022).
2. Han, Z.-H., Qiao, J.-L., Ding, Y.-L., Wang, G., Song, B.-F., Song, W.-P.: Key technologies for next-generation environmental-friendly supersonic transport aircraft: a review of recent progress. Acta Aerodynamica Sinica. 37(04), 620-635 (2019).
3. Morgenstern, J., Norstrud, N., Stelmack, M., Jha, P.: Advanced concept studies for supersonic commercial transports entering service in 2030-35 (N+3). In: 28th AIAA Applied Aerodynamics Conference. AIAA, Chicago, Illinois (2010).
4. Ding, Y.-L., Han, Z.-H., Qiao, J.-L., Nie, H., Song, W.-P., Song, B.-F.: Research progress in key technologies for conceptual-aerodynamic configuration design of supersonic transport aircraft [J]. Acta Aeronauticaet Astronautica Sinica. 44(2): 626310-626310 (2023).
5. Maglieri, D.J., Bobbitt, P.J., Plotkin, K. J., Shepherd, K.P., Coen, P.G., Richwine, D.M.: Sonic boom: Six decades of research. Technical Report, NASA/SP-2014-622 (2014).
6. Liebhardt, B., Lütjens, K., Ueno, A., Ishikawa, H.: JAXA's S4 Supersonic Low-Boom Airliner – A Collaborative Study on Aircraft Design, Sonic Boom Simulation, and Market Prospects. In: AIAA Aviation 2020 Forum. AIAA, Virtual Event (2020).
7. Li, W., Geiselhart, K.: Multidisciplinary design optimization of low-boom supersonic aircraft with mission constraints. AIAA Journal. 59(1), 165–179 (2021).
8. Ding, Y.-L., Han, Z.-H., Qiao, J.-L., Chen, Q., Song, W.-P., Song, B.-F.: Inverse design method for low-boom supersonic transport with lift constraint. AIAA Journal. 61(7), 2840–2853 (2023).
9. Doebler, W.J., Wilson, S.R., Loubeau, A., Sparrow, V.W.: Simulation and regression modeling of NASA's X-59 low-boom carpets across America. Journal of Aircraft. 60(2), 509–520 (2023).
10. Ding, Y.-L., Han, Z.-H., Qiao, J.-L., Song, W.-P., Song, B.-F.: Fast method and an integrated code for sonic boom prediction of supersonic commercial aircraft. In: 32nd ICAS Congress. Congress of the International Council of the Aeronautical Sciences, Shanghai, China (2021).
11. Whitham, G.: The fow pattern of a supersonic projectile. Communications on Pure and Applied Mathematics. 5(3), 301–348 (1952).
12. Walkden, F.: The shock pattern of a wing-body combination, far from the fight path. Aeronautical Quarterly. 9(2), 164–194 (1958).
13. Qiao, J.-L., Han, Z.-H., Zhang, L.-W., Song, W.-P., Song, B.-F.: Far-field sonic boom prediction considering atmospheric turbulence effects: An improved approach. Chinese Journal of Aeronautics. 35(9), 208–225 (2022).
14. Qiao, J.-L., Han, Z.-H, Song, W.-P, Song, B.-F.: Development of sonic boom prediction code for supersonic transports based on augmented Burgers equation. In: AIAA Aviation 2019 Forum. AIAA, Dallas, Texas (2019).
15. Stevens, S.S.: Perceived level of noise by Mark VII and decibels (E). The Journal of the Acoustical Society of America. 51(2), 575–601 (1972).
16. Jones, L.B.: Lower bounds for sonic bangs. The Aeronautical Journal. 65(606), 433-436 (1961).
17. Seebass, R.: Minimum sonic boom shock strengths and overpressures. Nature. 221(5181), 651-653 (1969).
18. George, A., Seebass, R.: Sonic boom minimization including both front and rear shocks. AIAA J. 9(10), 2091–2093 (1971).
19. Darden, C.M.: Sonic-boom minimization with nose-bluntness relaxation. Technical Report NASA Technical Paper 1348, NASA (1979).